Scientific and clinical implications of heterogeneity in uveal melanoma

Lange, M.J. de

3

Heterogeneity revealed by integrated genomic analysis uncovers a molecular switch in malignant uveal melanoma

Mark J. de Lange, Sake I. van Pelt, Mieke Versluis, Ekaterina S. Jordanova, Wilma G.M. Kroes, Claudia Ruivenkamp, Sjoerd H. van der Burg, Grégorius P.M. Luyten, Thorbald van Hall, Martine J. Jager, Pieter A. van der Velden

Oncotarget. 2015 Nov 10;6(35):37824-35.

ABSTRACT

Gene expression profiles as well as genomic imbalances are correlated with disease progression in uveal melanoma (UM). We integrated gene expression and genomic profiles to obtain insight into the oncogenic mechanisms in development and progression of UM. We used tumor tissue from 64 enucleated eyes of UM patients for profiling. Mutations and genomic imbalances were quantified with digital PCR to study tumor heterogeneity and molecular pathogenesis. Gene expression analysis divided the UM panel into three classes. Class I presented tumors with a good prognosis and a distinct genomic make up that is characterized by 6p gain. The UM with a bad prognosis were subdivided into class IIa and class IIb. These classes presented similar survival risks but could be distinguished by tumor heterogeneity. Class IIa presented homogeneous tumors while class IIb tumors, on average, contained 30% of non-mutant cells. Tumor heterogeneity coincided with expression of a set of immune genes revealing an extensive immune infiltrate in class IIb tumors. Molecularly, class IIa and IIb presented the same genomic configuration and could only be distinguished by 8q copy number. Moreover, UM establish in the void of the immune privileged eye indicating that in IIb tumors the infiltrate is attracted by the UM . Combined our data show that chromosome 8q contains the locus that causes the immune phentotype of UM. UM thereby provides an unique opportunity to study immune attraction by tumors.

INTRODUCTION

Uveal melanoma (UM) is a rare ocular neoplasm characterized by GNAQ and GNA11 mutations [1,2]. Despite changes in treatment, the overall survival rate remains low and patients still die due to metastases which are usually found after the initial diagnosis [3,4].

For years, monosomy of chromosome 3 has been the most described biomarker that predicts survival in UM patients[5]. Markers on chromosome 3 that underlie this unique subdivision are largely unknown but the chromosome 3 status divides UM genetically into two groups which have a good and a bad prognosis [6]. This finding is supported by clinical and histopathological markers [7]: UM containing epithelioid cells are associated with monosomy 3 and a bad prognosis while UM purely made up of spindle cells are rarely lethal[8,9]. Larger tumors are correlated with a worse prognosis and tend to have an epithelial/mixed phenotype rather than a spindle cell phenotype. With SNP [10–13], CGH [14–17] and karyotype analysis [18,19], recurrent chromosomal aberrations were further investigated in UM and shown to be correlated with disease progression. Gain of chromosome 8q and 6p is frequently detected while loss of 1p and 16q loss is less common but is still found to be correlated with prognosis [15,20,21]. Although these tumor characteristics can be applied to precisely predict disease outcome, we do not yet understand the sequence of genetic events in the development of UM, nor the relationship between the genetic changes and tumor behavior.

To better understand UM progression and develop targeted therapy, we performed genome-wide gene expression analysis and chromosome analysis of 64 tumors. We integrated gene expression and structural analysis to obtain insight into the molecular etiology of prognostic groups. We investigated prognostic genes and correlated them to chromosomal aberrations to visualize UM molecularly. Additionally, we validated structural aberrations with digital PCR (dPCR) which revealed the heterogeneity of UM. Cellular heterogeneity provides an insight into the microenvironment of UM while detailed molecular heterogeneity is the basis for a molecular progression model, showing that increased copy number of 8q precedes loss of chromosome 3. Moreover, our data show that distinct genetic events give rise to different classes of UM, impacting prognosis and therapy.

RESULTS

Expression profiles segregate UM into class I, IIa and IIb

Unsupervised cluster analysis of gene expression data of ~16,000 unique genes in 64 primary UM

subdivided the tumors into two distinct classes [22]. Class I tumors presented a good prognosis while class II tumors were correlated with a bad prognosis similar to what has been shown previously (Figure S1) [6]. Out of the 4,000 differentially expressed genes, 237 genes met the criteria of a Log fold change (LFC) of at least 1.0 and a p-value less than 0.05. A total of 132 genes presented a lower expression in class I than in class II, while the remaining 105 displayed a higher expression in class I. When using these 237 differentially expressed genes for cluster analysis, the UM cohort split into 3 clusters. Class I remained the same as with unsupervised analysis, but class II was subdivided into class IIa and IIb (Figure 1a).

Supervised gene expression analysis for IIa and IIb revealed a select panel of genes (n=53) that was differentially expressed between class IIa and IIb (Table S2). Among these genes, only two genes showed a higher expression in class IIa compared to IIb while 51 genes showed a higher expression in IIb (Figure 1b). Survival analysis revealed no significant difference between class IIa and IIb (not shown).

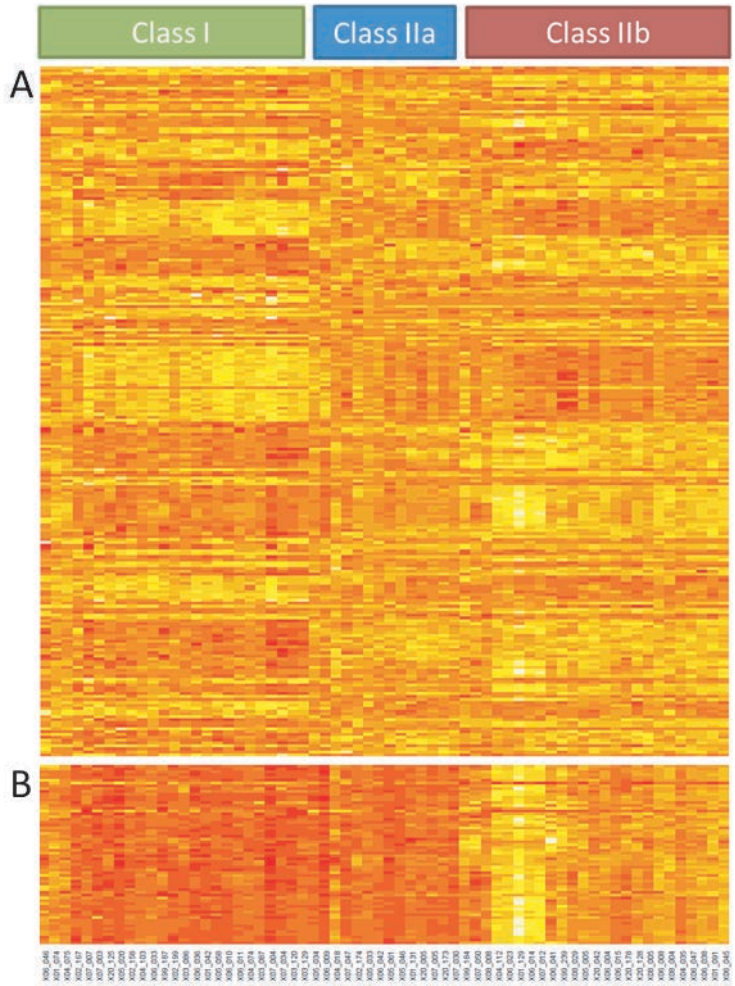

Figure 1. Gene expression analysis.
Unsupervised clustering of gene expression of 64 UM divides tumors in two classes. Supervised cluster analysis with the 237 most differentially expressed genes resulted in 3 classes because class II is subdivided in class IIa and class IIb (A). Supervised clustering of the 53 class IIb classifier genes (B).

Chromosomal aberrations are specific for UM classes

In order to investigate which genetic mechanisms underlie the subdivision into 3 classes, we investigated genomic aberrations in UM. With SNP analysis, five recurring chromosomal aberrations were detected which were validated with dPCR (Table 1). Loss of chromosome 1p, loss of chromosome 3, gain of chromosome 6p, gain of chromosome 8q and loss of chromosome 16q were common events. The distribution of the chromosomal aberrations

(Figure 2) as well as their copy numbers (Table S3) were plotted for the three classes showing that the chromosomal aberrations are non-randomly distributed over the three classes.

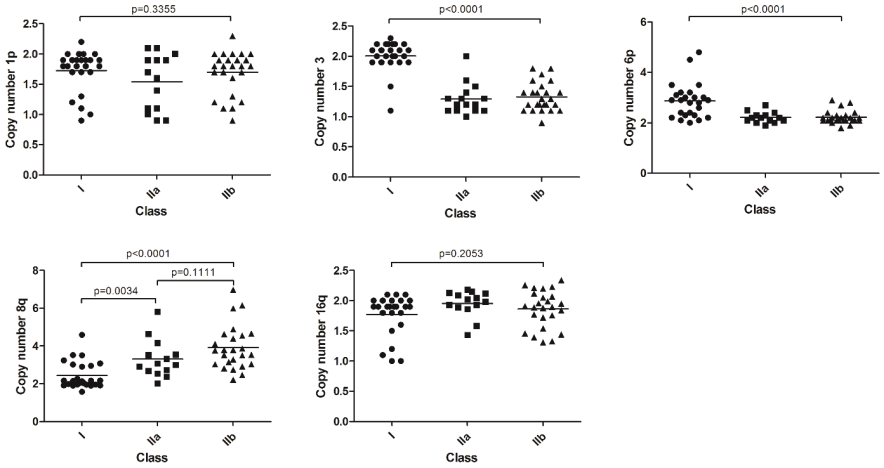

Figure 2. Chromosomal aberrations in expression classes.
Five recurrent abnormalities distributed over the gene expression classes. Differences between class I and II were mostly seen in chromosome 3 and 6. Gain of chromosome 8q appears to be the best classifier for IIa and IIb subdivision. Non-significant trends were seen in chromosome 1p and 16q.

Table 1, Copy number analysis. Copy number values of 64 UM measured with both SNP and dPCR analysis. Fractional abundance (FA) denotes the fraction of mutant alleles.

Class	Tumor no.	FA	Chr 1		Chr 3		Chr 6p		Chr 8q		Chr 16q	
		GNAQ/11	*dPCR*	*SNP*	*dPCR*	*SNP*	*dPCR*	*SNP*	*dPCR*	*SNP*	*dPCR*	*SNP*
I	06-046*	35.0**	1.7	2.0	2.0	1.9	2.7	2.6	2.7	2.7	1.4	1.3
I	01-074	48.9	1.2	1.4	2.2	1.9	2.9	2.0	3.5	2.7	2.1	2.3
I	04-075	37.1	1.8	1.7	2.0	1.9	2.8	1.9	3.0	2.9	2.0	2.0
I	02-167	45.1	1.3	1.5	1.5	1.6	2.3	2.1	2.1	2.1	2.0	2.0
I	07-007	36.8	1.7	1.9	1.1	1.0	2.9	2.8	1.9	1.9	2.0	1.8
I	07-003	37.9	1.1	1.0	2.2	2.0	2.2	2.0	2.2	1.9	1.9	1.8
I	20-125	38.5	2.0	1.9	2.2	2.0	4.8	2.1	3.2	2.7	1.9	1.9
I	05-020	34.3	1.0	1.2	1.9	1.9	3.5	3.4	4.6	4.5	1.0	1.1
I	02-158	40.2	2.0	2.0	2.3	2.0	4.5	1.6	2.2	2.0	1.5	1.6
I	04-103	44.8	1.8	1.9	1.9	2.0	2.9	1.3	1.9	2.0	1.9	2.1
I	06-033	46.7	0.9	1.1	2.1	2.1	3.0	3.1	3.0	3.2	1.0	1.0
I	99-187	43.2	1.9	1.9	2.2	2.0	2.2	2.0	2.2	2.0	1.1	1.6
I	02-199	42.2	2.0	1.7	2.0	1.8	2.4	2.2	2.0	1.9	2.0	1.9

Table 1, Copy number analysis. Copy number values of 64 UM measured with both SNP and dPCR analysis. Fractional abundance (FA) denotes the fraction of mutant alleles. (continued)

Class	Tumor no.	FA	Chr 1		Chr 3		Chr 6p		Chr 8q		Chr 16q	
		GNAQ/11	*dPCR*	*SNP*	*dPCR*	*SNP*	*dPCR*	*SNP*	*dPCR*	*SNP*	*dPCR*	*SNP*
I	03-086	53.8	1.9	1.9	2.2	2.0	2.3	2.0	2.0	1.9	2.1	2.0
I	06-036	47.4	1.9	2.0	2.2	2.0	3.2	3.1	2.9	3.1	2.1	1.9
I	01-042	50.0**	1.8	1.8	2.1	2.0	2.1	2.1	1.9	1.9	2.0	2.0
I	05-058	49	1.8	2.0	1.9	2.0	2.8	2.8	1.9	1.9	1.8	1.9
I	06-010	41.2	1.7	1.9	2.0	2.0	2.4	2.2	2.0	2.0	1.9	1.8
I	06-011	43	2.2	2.0	2.1	2.0	3.5	2.9	3.5	3.2	1.2	1.2
I	03-087*	44.4	1.7	1.9	2.0	2.1	2.4	2.1	1.9	2.0	1.6	1.8
I	04-074	48.5	1.8	2.2	1.9	2.0	3.0	2.1	2.0	2.0	1.9	2.0
I	07-004	33.6	1.9	1.9	2.1	2.1	3.2	3.2	2.0	2.0	1.8	1.8
I	07-034	46.7	1.7	2.0	2.0	1.9	3.0	2.8	2.1	2.0	1.9	1.9
I	03-120	52	1.9	1.9	2.0	2.0	3.1	2.8	1.9	1.9	1.9	1.8
I	03-129	29.5	1.9	1.9	1.4	1.5	2.0	2.1	3.1	2.7	1.9	1.6
IIa	05-034	36.4	1.6	1.6	1.6	1.5	2.2	2.2	3.1	3.1	1.6	1.5
IIa	06-009	49	1.1	1.1	1.0	1.1	2.5	2.3	3.0	3.2	1.9	2.1
IIa	04-018	55.4	1.9	2.0	2.0	1.9	2.7	2.0	2.7	2.3	1.9	1.9
IIa	07-047	24.3	0.9	1.0	1.1	1.0	2.0	2.0	2.0	2.0	1.9	1.8
IIa	02-174	47.3	0.9	1.3	1.1	1.4	2.1	2.2	2.7	2.6	2.0	2.1
IIa	05-033	45.7	1.4	1.5	1.2	1.1	2.0	1.9	2.4	2.1	2.2	1.9
IIa	06-042	34	1.9	1.9	1.3	1.1	2.2	2.1	2.9	3.0	2.0	1.9
IIa	05-061	45.2	1.0	1.1	1.1	1.0	2.2	2.0	5.8	5.7	2.1	1.9
IIa	05-046	43.1	1.1	1.1	1.1	1.1	2.1	1.9	3.5	3.7	1.9	1.9
IIa	01-131	35.5	2.1	2.1	1.5	1.5	2.3	2.1	4.6	3.4	1.4	1.6
IIa	20-005	45.6	1.9	2.0	1.2	1.4	2.3	2.1	3.3	2.9	2.1	2.2
IIa	07-005	42.9	1.7	1.9	1.3	1.3	1.9	2.3	4.2	3.9	2.0	1.9
IIa	20-173	43.7	2.0	1.9	1.3	1.3	2.4	2.1	2.5	2.3	2.2	2.3
IIa	07-030	44.5	2.1	2.0	1.2	1.1	2.1	2.0	3.5	3.2	2.1	1.9
IIb	99-184	36.7	1.8	2.0	1.4	1.5	2.1	1.9	4.4	3.3	1.4	1.7
IIb	08-008	39.5**	2.0	1.9	1.2	1.1	2.1	2.0	2.9	2.7	2.2	1.8
IIb	07-050	37.1	1.1	1.2	1.2	1.1	2.1	2.0	4.9	4.9	2.1	2.0
IIb	04-112	44.3	1.7	2.0	1.1	1.3	1.9	2.1	3.5	3.5	1.9	2.0
IIb	06-023	31.5	1.9	2.0	1.4	1.3	2.1	2.1	2.5	2.6	1.9	1.9
IIb	01-129	12.8	1.9	2.0	1.8	1.8	2.1	2.1	2.2	2.1	2.0	2.0
IIb	06-014	19.8	2.0	2.0	1.8	1.6	2.4	2.2	4.7	4.5	1.8	1.6
IIb	07-012	15.8	2.0	1.9	1.7	1.5	2.3	2.0	3.8	3.7	2.2	2.0

Table 1, Copy number analysis. Copy number values of 64 UM measured with both SNP and dPCR analysis. Fractional abundance (FA) denotes the fraction of mutant alleles. (continued)

Class	Tumor no.	FA	Chr 1		Chr 3		Chr 6p		Chr 8q		Chr 16q	
		GNAQ/11	*dPCR*	*SNP*	*dPCR*	*SNP*	*dPCR*	*SNP*	*dPCR*	*SNP*	*dPCR*	*SNP*
IIb	06-041	42	1.8	1.9	1.3	1.2	2.2	2.0	4.6	4.7	1.9	1.8
IIb	99-239	43.4	1.6	1.8	0.9	1.4	1.8	1.9	3.5	3.3	1.3	1.9
IIb	08-029	40.4	1.1	1.3	1.3	1.2	2.1	2.1	3.5	3.2	2.2	1.9
IIb	05-005	21.9	1.7	1.9	1.4	1.3	2.0	2.0	3.1	3.2	1.8	1.8
IIb	20-042	35.9	1.8	1.6	1.6	1.5	2.9	1.9	3.9	3.1	2.3	2.0
IIb	06-004	43.5	1.9	2.1	1.1	1.1	2.1	2.0	3.8	4.2	1.8	1.9
IIb	20-178	27.3	0.9	1.2	1.1	1.3	2.1	2.0	6.0	4.2	1.9	2.1
IIb	06-015	44	1.2	1.3	1.2	1.0	2.3	2.1	3.8	3.9	2.1	1.9
IIb	20-128	39.3	2.3	2.0	1.5	1.5	2.7	1.6	6.2	3.9	1.4	1.7
IIb	08-005	27.4	1.3	1.4	1.2	1.3	2.4	2.0	7.0	5.7	1.3	1.3
IIb	06-008	36.3	1.2	1.1	1.4	1.2	2.2	2.0	3.0	2.9	2.3	1.9
IIb	08-004	33.5**	1.7	1.9	1.2	1.2	2.8	2.8	2.8	2.8	2.0	1.8
IIb	04-035	43	1.8	2.1	1.1	1.3	2.1	2.2	3.0	2.7	2.0	1.9
IIb	06-047	35.8	2.0	1.9	1.4	1.2	2.2	2.0	2.7	2.8	2.1	1.8
IIb	06-038	39.6	2.0	2.1	1.1	1.1	2.2	2.1	3.3	3.4	1.5	1.4
IIb	01-091	44	1.9	2.0	1.2	1.4	2.1	2.1	4.6	3.8	1.5	1.7
IIb	06-045	31.1	1.8	1.8	1.6	1.5	2.2	2.0	4.1	3.8	1.7	1.5

** Chromosome 5 imbalance, TTC5 copy number used as reference.*
*** FA values were calculated with copy number analysis.*

Chromosome 3 loss and gain of 6p define tumor class

Loss of chromosome 3 was predominantly presented in class II (a/b) tumors and was only detected in 3 out 25 class I tumors (table S3). In contrast, gain of chromosomal part 6p was most prominent in class I tumors. Moreover, co-occurrence of 6p gain and monosomy 3 in UM was rare and 6p copy number was low in these instances, marginally exceeding the thresholds for gain (Figure 3).

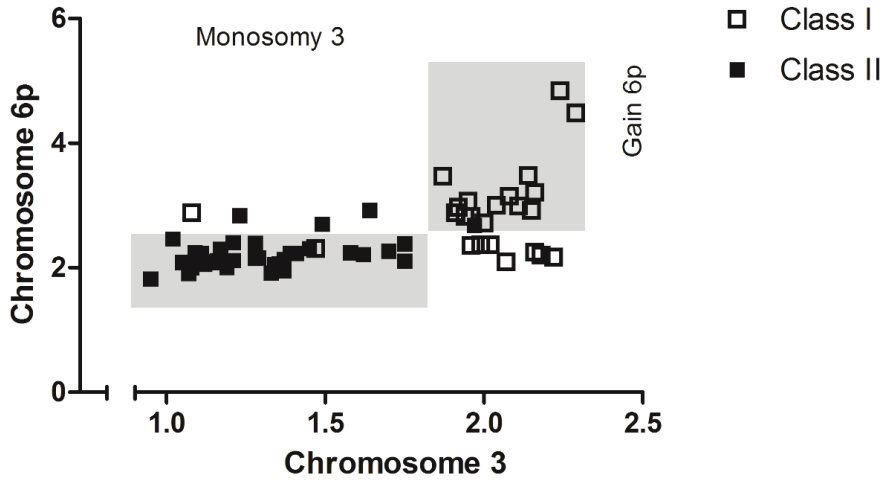

Figure 3. Chromosomal anomalies support UM subdivision.
Monosomy 3 and 6p gain divided UM in class I and class II. In the mixed tumors 6p copy number was low.

Increased 8q copy number in class IIb tumors

Monosomy 3 and 6p gain molecularly characterize class II and class I tumors, respectively, but do not differentiate class IIa from class IIb tumors. However with analysis of the aberrations of 8q and to a lesser extent 16q this turned out to be possible. Class IIb tumors presented a higher 8q copy number than class IIa tumors (Figure 2). Moreover, the mechanism underlying gain of 8q was different in these two UM classes. Amplification of 8q observed in class IIb was almost exclusively caused by isochromosome formation. The limited gain of 8q that was observed in class IIa tumors was more often due to gain of the entire chromosome [23]. Loss of 16q was not significantly differentially distributed over the three UM classes.

Functional and genetic annotation

To investigate the link between chromosomal aberrations and differentially expressed genes we analyzed potential genetic and functional correlations of the 237 top differentially expressed genes (Figure 1). Functional annotation showed that 6 terms were significantly overrepresented in the 237 genes (Table 2). These terms concerned the immune system (n=4) and the translation machinery (n=2).

Table 2, functional annotation of classifier genes. Functional annotation of the most differentially expressed genes between class I and II. After correction for multiple testing, 6 terms were found to be significantly overrepresented.

Term	Count	Bonferroni	Class
Antigen processing and presentation	16	5.8E-11	IIa-IIb
Immune response	34	6.7E-09	IIa-IIb
Translational elongation	15	1.8E-08	I-II
Antigen processing and presentation of peptide antigen	10	3E-08	IIa-IIb
Antigen processing and presentation of peptide antigen via MHC class I	7	0.000039	IIa-IIb
Translation	19	0.00011	I-II

Among the 237 genes we identified 151 genes that define the difference between class I and class II in general (Table S2). These genes were differentially expressed (LFC >1 or LFC<-1; p<0.05) between class I and class II but did not significantly differ between class IIa and IIb. Genes on chromosome 3 and 6 were overrepresented with respectively 16 and 12 genes. All of the 16 genes from chromosome 3 showed a lower expression in class II tumors compared to class I tumors corresponding to loss of chromosome 3 in class II. In contrast, the 12 genes on 6p showed either an elevated or a decreased expression in class II. Functional annotation of the differentially-expressed genes showed that the terms all concerned ribosomal and other translational machinery proteins (Table 2).

The class IIb classifier genes are involved in the immune response

Next, the genes differentially-expressed between class IIa and IIb tumors were annotated. In total, 53 genes were significantly differentially expressed (LFC >1 or <-1; p<0.05) between class IIa and IIb tumors but did not differ between class I and IIa tumors (Table S2). There was no clustering of genes to chromosome 8q or 16q. Remarkably, 26 genes on chromosome 6, many of which are involved in the immune response, revealed a significant overrepresentation. Of the 26 genes located on chromosome 6, a significant part is involved in HLA/T-cell reactions. Moreover, many of the genes that define class IIb, appear to be targets of interferon. These data suggest that part of the different gene expression between class IIb and class I and IIa tumors may be due to tumor-resident non-cancer cells.

Tumor heterogeneity in UM

Based on the assumption that every tumor cell within a mutant UM I either carries a GNAQ or GNA11 mutation we were able to calculate the fractional abundance (FA), which represents the ratio between cancer cells and non-cancer cells (e.g. fibroblasts, immune cells) within the tumor. Four tumors did not present one of the hotspot mutations in GNAQ/11 when analyzed with dPCR and in these cases the monosomy 3 status was used

to calculate the FA. This was warranted by the positive correlation between tumor fraction calculated with GNAQ/GNA11 mutation and monosomy 3 (Figure S2).

Figure 4a shows the fraction of tumor cells and their distribution over the three classes. No significant difference was found between class I and IIa but a significantly decreased tumor cell percentage was detected in class IIb tumors, sustaining the previous notion that the different chromosome 6 associated gene expression in class IIb tumors may be due to non-tumor cells. As the copy number of the aberrations in this study is the result of admixture of normal cells and tumor cells, we also calculated corrected copy numbers. Fractional abundance of tumor cells was used for a more precise calculation of chromosome 8q copy numbers in the tumor cells (Figure 4b). The mean 8q copy number after adjustment in class I, class IIa and class IIb, was 2.6, 3.5 and 5.0, respectively. For the other aberrations, a dosage effect is not clinically relevant, and therefore we did not calculate adjusted copy numbers.

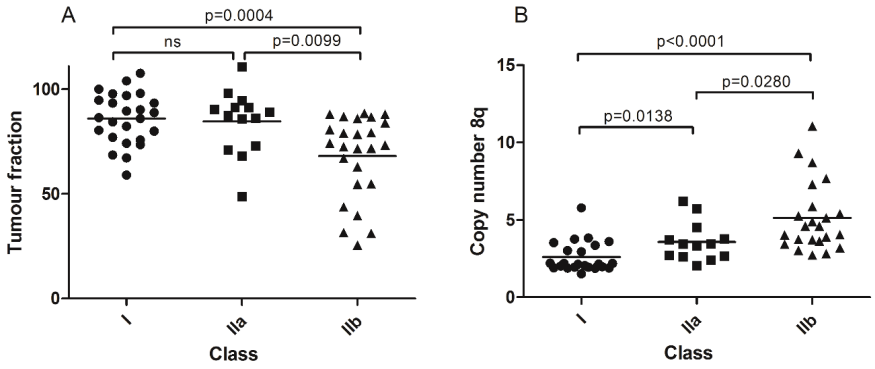

Figure 4. Quantification of tumor heterogeneity.
Tumor fractions based on GNAQ/11 mutation analyzed with dPCR. Class IIb contains tumors with a significantly lower tumor fraction (A). After adjusting chromosome 8q copy number for tumor fraction, significant differences were also found between class IIa and class IIb besides the significant differences between class I and class II (B).

Genetic heterogeneity in UM revealed clonal evolution

Tumor heterogeneity was also determined with fractional abundance of the chromosomal imbalances. Moreover, quantification of tumor heterogeneity with dPCR provided information on the sequence of events. In UM 20-042 for example, 71.8% of the cells contained the GNAQ Q209P mutation while a chromosome 3 copy number of 1,64 indicated that 36% of the cells contained monosomy 3 and thereby revealed that monosomy 3 occurred after GNAQ mutation (Table 1). Because 8q copy number in UM varied widely we used karyotyping to order monosomy 3 and 8q gain instead (Figure 5a). Among 39 UM

with monosomy 3 and 8q gain, three tumors (20-173, 06-015 and 06-023) displayed 8q gain in all tumor cells, but some cells contained two copies of chromosome 3. This indicates that 8q gain occurred before monosomy 3 in these tumors.

With dPCR calculated tumor fractions we furthermore deduced that loss of 16q seems to be more common as a quaternary event following monosomy 3. Ultimately, 1p loss occurs as the last event in this series of five recurrent aberrations (Figure 5b). For monosomy 3 and chromosome 16q loss, 14 tumors showed heterogeneity (ΔX>0.2) and all showed a larger monosomy 3 tumor fraction. For the combination of loss of 16q and 1p, only six UM were informative and all showed a higher 16q tumor fraction compared to the 1p fraction. Temporal distribution of chromosomal aberrations can also be determined with the number of imbalances in a tumor and this was applied for 6p gain [24]. In class I, three UM presented only one imbalance and in all of these cases it concerned 6p gain. This indicated that in class I tumors, 6p gain most likely occurred first, following the GNAQ/11 mutation (Figure 5c).

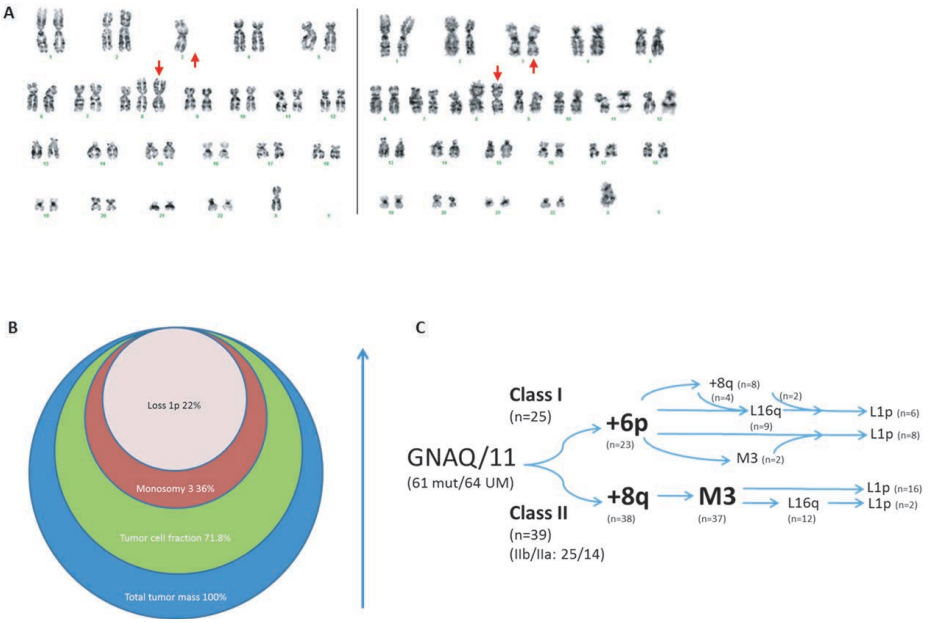

Figure 5. Chronology of genomic imbalances in UM development.
Karyograms of 06-023 revealed monosomy 3 heterogeneity while homogeneous isochromosome 8q indicated that it preceded monosomy 3 (A). UM 20-042 displayed heterogeneity for monosomy 3 and loss of 1p, indicated by circles that represent the fractions of the tumor containing a specific chromosomal aberration (B). Integration of tumor heterogeneity with gene-expression classes suggested distinct chronology in UM development in class I and class II (C). Two UM in class I did not contain 6p gain but presented L1p and M3/8q+ genotypes respectively. The class II UM without gain of 8q did present monosomy 3.

DISCUSSION

For UM excellent molecular markers exist to predict disease outcome [25]. Chromosomal imbalances and gene expression profiles accurately predict disease progression in UM but so far have not resulted in improved treatment. We set out to integrate expression and genomic profiles of UM to study the underlying mechanisms as this may facilitate a knowledge based treatment. By applying a rigorous data reduction to the gene expression analysis, we revealed three expression classes. These classes overlapped with classes that were identified by unsupervised cluster analysis but divided the UM with a bad prognosis into two groups that were designated class IIa and class IIb. The immune response and the translation machinery were the only two functions significantly enriched among the 237 genes that defined the three classes.

The five recurrent aberrations that were analyzed, were non-randomly distributed over the expression classes. In our tumor set, monosomy 3 and 6p gain clearly divided the tumors into class I and class II (a/b) (Figure 3). Based on the fact that monosomy 3 and 6p gain are present in different UM it is commonly assumed that these aberrations are mutually exclusive [26–28]. Quantification with digital PCR however showed some degree of 6p gain in combination with monosomy 3 and thereby indicates that the mutual exclusivity is not absolute. Though, our observations suggest that tumor clones presenting both monosomy 3 and 6p gain are unsuccessful and remain small. Class IIa and class IIb can be distinguished with 8q copy number. The number of chromosome 8q copies is highest in class IIb and this was related to a different underlying mechanism between classes. Class IIa more commonly yielded tumors with gain of a complete chromosome 8 while class IIb tumors almost exclusively displayed 8q copy gains due to isochromosome formation [23]. The formation of chromosome 8q isochromosomes is a phenomenon earlier described in UM [29–31].

Remarkably, most of the genes highly expressed in class IIb tumors are involved in immune regulation and located on chromosome 6 which is rarely gained in class II tumors. We therefore postulated that these differentially-expressed genes were not the result of differences in tumor cells, but expressed by stromal cells (e.g. fibroblasts and immune cells). This notion was sustained by our calculation of the tumor cell fraction in the total tumor mass. The tumor cell percentage was similar between class I and class IIa but was significantly lower in class IIb tumors suggesting a higher percentage of non-cancer cells in class IIb tumors. The role of the immune system in UM development has not yet been elucidated but correlations with survival and other prognostic markers have been made [32–34]. In UM, a bad prognosis is correlated with the presence of immune infiltrate [33] and an immune infiltrate may be what is causing the expression profile of class IIb (table 2).

Importantly class IIa tumors, that present a high tumor percentage leaving few space for immune cell infiltrate, are also correlated with a bad prognosis. This implies that that the immune cells are not a prerequisite for the class IIa tumors to progress and metastasize.

The calculated tumor percentages of each chromosome loss furthermore allowed us to deduce the sequence of events in UM. Based on dPCR analysis we calculated which percentage of cells contained specific chromosomal losses (Figure 2). Because chromosomal gains could not be used to determine fractional abundance we used alternative approaches for 6p gain and 8q gain. In class I tumors 6p aberrations appear to occur first based on the fact that 22 out of 25 UM presented 6p gain in this class and because the tumors with only one chromosomal imbalance all presented 6p gain. Previous reports suggest that loss of chromosome 3 precedes the addition of 8q [35] but cytogenetic analysis of informative UM in our dataset supported the opposite. Karyotyping revealed monosomy 3 heterogeneity in tumors that are homogeneous for 8q gain and thereby suggested that chromosome 8q imbalance occurs prior to monosomy 3 in class II tumors. With regard to the sequence of chromosomal losses, we deduced that monosomy 3 occurs first, followed by loss of 16q and loss of 1p respectively

Surprisingly for such an early event, 8q copy number made molecular discrimination of the three gene-expression classes possible when we adjusted chromosome 8q copy number for tumor fraction. In a dosage-dependent manner, significant differences were revealed between the three expression classes. Previous studies showed that 8q copy number correlates with survival but no significant survival differences were revealed between class IIa and class IIb even though 8q copy number differed between these classes (Figure 4b). Both expression differences and genomic differences nevertheless suggest that class IIa and IIb represent different entities that may require different treatments.

In short, with integrated analysis of gene expression and genomic aberrations we were able to distinguish three molecular classes in UM. Based on an apparent immune infiltrate in class IIb we hypothesize that class II can progress either with or without immune involvement. Defining these classes gives us the opportunity to investigate the mechanism behind immune involvement in UM. Chromosome 8q is likely to be a candidate locus to search for targets since it is differentially changed in class IIa compared to class IIb. Dividing UM on a molecular level reveals tumor diversity and can lead to new possibilities for therapeutic intervention.

MATERIALS AND METHODS

We used tumor material from 64 enucleated eyes of uveal melanoma patients that had been enucleated at the Leiden University Medical Center, Leiden, The Netherlands, between 1999 and 2008. Written informed consent was obtained for all patient samples. None of the tumors had prior treatment and we only used tumors with a follow-up time of at least 4 years. The maximum follow-up was 14 years. The average age at enucleation was 60.6 years (range 13 to 88); 33 patients were male and 31 female.

Tumor material was snap frozen using 2-methyl butane and RNA and DNA was isolated using the RNeasy mini kit and QIAmp DNA minikit, respectively, (both Qiagen, Valencia, USA) from 20 sections of 20µm according to the manufacturer's guidelines.

Gene expression profiling

Gene expression was determined using the Illumina HumanHT-12 v4 chip containing 47,000 probes across the whole genome that will be referred to as genes in the remainder of the text. Genes in the supervised cluster analysis with a log-fold change (LFC) larger than 1 or smaller than -1 and a p-value smaller than 0.05 were labelled "significantly differentially expressed". For differences between subgroups i.e. I versus II, we corrected for differences between IIa and IIb classified as LFC smaller than -0.5 or greater than 0.5 and a p-value smaller than 0.05. These most differentially-expressed genes were annotated and biological processes were analyzed using the Database for Annotation, Visualization and Integrated Discovery (DAVID) [36,37].

SNP analysis

SNP microarray analysis was used to determine chromosomal aberrations. Two types of SNP microarray chips were used, the Affymetrix 250K_NSP-chip, with ~250,000 probes across the genome and the Affymetrix Cytoscan HD chip, with ~750,000. The first 28 samples were analyzed with the Affymetrix 250K_NSP chip, and the remaining 36 samples with the Affymetrix Cytoscan HD chip. Analysis of the Affymetrix 250K_NSP chips was performed with the 'Genotyping Console' to determine the copy number values and the 'GCT Browser' to visualize the data (both from Affymetrix, Santa Clara, USA). Affymetrix Cytoscan HD chips were analyzed with 'ChAS'. Different loci per chromosome were evaluated to adjust for partial gains or deletions. ~200 probes per gene locus were averaged to determine eventual copy number.

dPCR

Copy number analysis

The copy number of chromosome 1p, 3, 6p, 8q, and 16q was determined using probes for CDC42, *PPARG*, *NEDD9*, *PTK2*, and *NFAT5* respectively. For calculation of normalized copy numbers, out of 3 control probes located on chromosome 5, 7, and 14 (*TERT*, *VOPP1* and *TTC5*), *TERT* (situated at chromosome 5), was selected based on stability in this tumor set. In the two cases with chromosome 5 gain we used *TTC5* as reference to calculate the copy numbers. Thresholds for copy number analysis were: loss, <1.9: normal, 1.9-2.1: gain, >2.1-<3.1: amplification, >3.1 (method described by Versluis et al. [23]). In short, 50-60ng of DNA of each sample was used in a 20ul reaction volume. Reaction mixture consisted of 2x droplet PCR supermix (Bio-Rad Laboratories, Inc., Hercules, USA), 20x target probe (FAM), 20x reference probe (HEX). Sequence context is provided in supplemental table S1. Droplets were generated using a QX100 droplet generator and after the PCR, the plate was loaded into the QX100 droplet reader (both Bio-Rad Laboratories, Inc.). The following end point PCR protocol using a T100 thermal cycler was used: 95oC, 10min; (94oC, 30sec; 60oC, 1min) 40x; 98oC, 10min; 4oC, till end. Digital PCR (dPCR) software (QuantaSoft) reads the positive and negative droplets in each sample and plots the fluorescence droplet by droplet. Fractional abundance was calculated as $FA = \frac{mutant\ amplicons}{mutant\ amplicons\ +\ wildtype\ amplicons}$. The positive droplets represent the concentration of the target allele in the sample. Corrections made for the fraction of tumor cells containing chromosomal aberrations (Z) based on FA were performed as follows: X represents the dPCR value for copy number of chromosome n, and Y represents the tumor fraction of the associated tumor which is calculated by multiplying the FA by 2.

Heterogeneity of imbalances was determined by subtracting copy numbers and a difference of 0.2 copy number was used as threshold (ΔX>0.2).

$$Z = \frac{X - (2\left(1 - \left(\frac{Y}{100}\right)\right))}{\frac{Y}{100}}$$

GNAQ/11 mutation detection

GNAQ and GNA11 mutations were detected using hydrolysis probes in a multiplex dPCR. 10ng of sample DNA was used in a 20ul reaction volume. The reaction mixture consisted of 2x droplet PCR supermix (Bio-Rad Laboratories, Inc.), 20x target probe (FAM), and 20x wildtype probe (HEX). Proprietary probes and primers (Bio-Rad Laboratories, Inc.) were used and the sequence context is provided in supplemental table S1. Droplet generation, thermal cycling and reads were similar to the method described in the previous section.

PCR to end point protocol used: 95oC, 10min; (94oC, 30sec; 55oC, 1min) 40x; 98oC, 10min; 4oC, till end.

Karyotyping

Following enucleation, a small part of each tumor was sent out for cell culture. Following mechanical dissection of the tumor biopsy, cells were washed and placed into one flask with RPMI 1640 (15% fetal bovine serum [Invitrogen, Breda, The Netherlands]) medium and another flask with Amniochrome II (Cambrix Bio Science, Verviers, Belgium). The flasks were cultured at 37°C with 5% CO2 for up to 4 weeks and harvested when at least 75% of the surface was covered with cells (after a mean of 18 days; SD, 9.4 days). When cell culturing was successful, conventional karyotyping was performed, to determine the presence of chromosomal changes. Two independent observers assessed all evaluations and scores, each without knowledge of the results obtained by the other investigator, to ensure accuracy of quantification of the slides. In case of a difference, consensus was reached during a simultaneous session. Cytogenetic analysis was performed on GTG-banded (G-banding with trypsin and Giemsa) metaphases. In the case of a normal karyotype, at least 20 metaphases were analyzed. When an abnormal clone was detected in the first ten karyotyped cells, no further analysis was performed; when three cells with loss of 1 copy of chromosome 3 were observed, monosomy 3 was identified.

Statistical analysis

For gene expression analysis, the statistical programming language R was used (R: A Language and Environment for Statistical Computing, R Core Team, R foundation for Statistical Computing, Vienna, Austria, 2014). Since data have been obtained in two batches, a batch effect correction was applied. The R packages used were: 'ber' for batch correction and 'lumi' for unsupervised clustering. To compare survival between UM patients in different classes Kaplan-Meier functions were plotted. Survival analysis was performed using the log-rank test. The Pearson's correlation test was used to assess the correlation between the fraction of tumor cells containing GNAQ/11 and the fraction of tumor cells containing chromosome 3 aberrations. The Chi square test was used to test frequency differences in chromosomal aberrations in different subgroups. Likelihood ratios were used for cases in which the Chi square assumption was violated. α=0.05 was used as threshold for significance in all tests. For statistical analysis SPSS V.20.0.1 (IBM SPSS statistics, IBM corporation, Armonk, New York, USA) was used.

ACKNOWLEDGEMENTS

The authors thank Ronald van Eijk from the Department of Pathology of the LUMC for helpful discussion. Eddy van Collenburg and Roy Wiggers (BioRad Laboratories) for providing probes and primers. Guido J.E.J. Hooiveld (WU Agrotechnology & Food Sciences) for use of the digital PCR facility and Frank de Gruijl for his expertise in mathematics.

[1] Van Raamsdonk CD, Bezrookove V, Green G, Bauer J, Gaugler L, O'Brien JM, et al. Frequent somatic mutations of GNAQ in uveal melanoma and blue naevi. Nature. 2009;457(7229):599–602. https://doi.org/10.1038/nature07586.

[2] Van Raamsdonk CD, Griewank KG, Crosby MB, Garrido MC, Vemula S, Wiesner T, et al. Mutations in GNA11 in uveal melanoma. N Engl J Med. 2010;363(23):2191–9. https://doi.org/10.1056/NEJMoa1000584.

[3] Eskelin S, Pyrhönen S, Summanen P, Hahka-Kemppinen M, Kivelä T. Tumor doubling times in metastatic malignant melanoma of the uvea: Tumor progression before and after treatment. Ophthalmology. 2000;107(8):1443–9. https://doi.org/10.1016/S0161-6420(00)00182-2.

[4] Singh AD, Turell ME, Topham AK. Uveal melanoma: Trends in incidence, treatment, and survival. Ophthalmology. 2011;118(9):1881–5. https://doi.org/10.1016/j.ophtha.2011.01.040.

[5] Prescher G, Bornfeld N, Hirche H, Horsthemke B, Jöckel KH, Becher R. Prognostic implications of monosomy 3 in uveal melanoma. Lancet. 1996;347(9010):1222–5. https://doi.org/10.1016/S0140-6736(96)90736-9.

[6] Onken MD, Worley LA, Ehlers JP, Harbour JW. Gene expression profiling in uveal melanoma reveals two molecular classes and predicts metastatic death. Cancer Res. 2004;64(20):7205–9. https://doi.org/10.1158/0008-5472.CAN-04-1750.

[7] Scholes AGM, Damato BE, Nunn J, Hiscott P, Grierson I, Field JK. Monosomy 3 in uveal melanoma: Correlation with clinical and histologic predictors of survival. Investig Ophthalmol Vis Sci. 2003;44(3):1008–11. https://doi.org/10.1167/iovs.02-0159.

[8] Seddon JM, Polivogianis L, Gragoudas ES, Hsieh CC, Albert DM, Gamel JW. Death From Uveal Melanoma: Number of Epithelioid Cells and Inverse SD of Nucleolar Area as Prognostic Factors. Arch Ophthalmol. 1987;105(6):801–6. https://doi.org/10.1001/archopht.1987.01060060087039.

[9] McLean IW, Foster WD, Zimmerman LE, Gamel JW. Modifications of Callender's classification of uveal melanoma at the Armed Forces Institute of Pathology. Am J Ophthalmol. 1983;96(4):502–9. https://doi.org/10.1016/S0002-9394(14)77914-0.

[10] Onken MD, Worley LA, Person E, Char DH, Bowcock AM, Harbour JW. Loss of heterozygosity of chromosome 3 detected with single nucleotide polymorphisms is superior to monosomy 3 for predicting metastasis in uveal melanoma. Clin Cancer Res. 2007;13(10):2923–7. https://doi.org/10.1158/1078-0432.CCR-06-2383.

[11] Lake SL, Coupland SE, Taktak AFG, Damato BE. Whole-genome microarray detects deletions and loss of heterozygosity of chromosome 3 occurring exclusively in metastasizing uveal melanoma. Investig Ophthalmol Vis Sci. 2010;51(10):4884–91. https://doi.org/10.1167/iovs.09-5083.

[12] McCannel TA, Burgess BL, Nelson SF, Eskin A, Straatsma BR. Genomic identification of significant targets in ciliochoroidal melanoma. Investig Ophthalmol Vis Sci. 2011;52(6):3018–22. https://doi.org/10.1167/iovs.10-5864.

[13] Singh AD, Aronow ME, Sun Y, Bebek G, Sauntharajah Y, Schoenfield LR, et al. Chromosome 3 status in uveal melanoma: A comparison of fluorescence in situ hybridization and single-nucleotide polymorphism array. Investig Ophthalmol Vis Sci. 2012;53(7):3331–9. https://doi.org/10.1167/iovs.11-9027.

[14] Gordon KB, Thompson CT, Char DH, O'Brien JM, Kroll S, Ghazvini S, et al. Comparative Genomic Hybridization in the Detection of DNA Copy Number Abnormalities in Uveal Melanoma. Cancer Res. 1994;54(17):4764–8.

[15] Trolet J, Hupé P, Huon I, Lebigot I, Decraene C, Delattre O, et al. Genomic profiling and identification of high-risk uveal melanoma by array CGH analysis of primary tumors and liver metastases. Investig Ophthalmol Vis Sci. 2009;50(6):2572–80. https://doi.org/10.1167/iovs.08-2296.

[16] Speicher MR, Prescher G, du Manoir S, Jauch A, Horsthemke B, Bornfeld N, et al. Chromosomal Gains and Losses in Uveal Melanomas Detected by Comparative Genomic Hybridization. Cancer Res. 1994;54(14):3817–23.

[17] Ghazvini S, Char DH, Kroll S, Waldman FM, Pinkel D. Comparative genomic hybridization analysis of archival formalin-fixed paraffin-embedded uveal melanomas. Cancer Genet Cytogenet. 1996;90(2):95–101. https://doi.org/10.1016/S0165-4608(96)00076-3.

[18] Naus NC, Van Drunen E, De Klein A, Luyten GPM, Paridaens DA, Alers JC, et al. Characterization of complex chromosomal abnormalities in uveal melanoma by fluorescence in situ hybridization, spectral karyotyping, and comparative genomic hybridization. Genes Chromosom Cancer. 2001;30(3):267–73. https://doi.org/10.1002/1098-2264(2000)9999:9999<::AID-GCC1088>3.0.CO;2-7.

[19] White JS, Becker RL, McLean IW, Director-Myska AE, Nath J. Molecular cytogenetic evaluation of 10 uveal melanoma cell lines. Cancer Genet Cytogenet. 2006;168(1):11–21. https://doi.org/10.1016/j.cancergencyto.2005.11.016.

[20] Sisley K, Parsons MA, Garnham J, Potter AM, Curtis D, Rees RC, et al. Association of specific chromosome alterations with tumour phenotype in posterior uveal melanoma. Br J Cancer. 2000;82(2):330. https://doi.org/10.1054/BJOC.1999.0923.

[21] White JS, McLean IW, Becker RL, Director-Myska AE, Nath J. Correlation of comparative genomic hybridization results of 100 archival uveal melanomas with patient survival. Cancer Genet Cytogenet. 2006;170(1):29–39. https://doi.org/10.1016/j.cancergencyto.2006.05.004.

[22] Tschentscher F, Hüsing J, Hölter T, Kruse E, Dresen IG, Jöckel KH, et al. Tumor classification based on gene expression profiling shows that uveal melanomas with and without monosomy 3 represent two distinct entities. Cancer Res. 2003;63(10):2578–84.

[23] Versluis M, De Lange MJ, Van Pelt SI, Ruivenkamp CAL, Kroes WGM, Cao J, et al. Digital PCR validates 8q dosage as prognostic tool in uveal melanoma. PLoS One. 2015;10(3):e0116371. https://doi.org/10.1371/journal.pone.0116371.

[24] Höglund M, Gisselsson D, Hansen GB, White VA, Säll T, Mitelman F, et al. Dissecting karyotypic patterns in malignant melanomas: Temporal clustering of losses and gains in melanoma karyotypic evolution. Int J Cancer. 2004;108(1):57–65. https://doi.org/10.1002/ijc.11558.

[25] Singh AD, Shields CL, Shields JA. Prognostic factors in uveal melanoma. Melanoma Res. 2001;11(3):255–63. https://doi.org/10.1097/00008390-200106000-00007.

[26] Bonaldi L, Midena E, Filippi B, Tebaldi E, Marcato R, Parrozzani R, et al. FISH analysis of chromosomes 3 and 6 on fine needle aspiration biopsy samples identifies distinct subgroups of uveal melanomas. J Cancer Res Clin Oncol. 2008;134(10):1123–7. https://doi.org/10.1007/s00432-008-0382-6.

[27] Parrella P, Sidransky D, Merbs SL. Allelotype of posterior uveal melanoma: implications for a bifurcated tumor progression pathway. Cancer Res. 1999;59(13):3032–7.

[28] Young TA, Burgess BL, Rao NP, Gorin MB, Straatsma BR. High-density genome array is superior to fluorescence in-situ hybridization analysis of monosomy 3 in choroidal melanoma fine needle aspiration biopsy. Mol Vis. 2007;13:2328–33.

[29] Prescher G, Bornfeld N, Friedrichs W, Seeber S, Becher R. Cytogenetics of twelve cases of uveal melanoma and patterns of nonrandom anomalies and isochromosome formation. Cancer Genet Cytogenet. 1995;80(1):40–6. https://doi.org/10.1016/0165-4608(94)00165-8.

[30] Horsman DE, Sroka H, Rootman J, White VA. Monosomy 3 and isochromosome 8q in a uveal melanoma. Cancer Genet Cytogenet. 1990;45(2):249–53. https://doi.org/10.1016/0165-4608(90)90090-W.

[31] Couturier J, Saule S. Genetic determinants of uveal melanoma. Dev Ophthalmol. 2012;49:150–65. https://doi.org/10.1159/000328270.

[32] De Waard-Siebinga I, Hilders CGJM, Hansen BE, Van Delft JL, Jager MJ. HLA expression and tumor-infiltrating immune cells in uveal melanoma. Graefe's Arch Clin Exp Ophthalmol. 1996;234(1):34–42. https://doi.org/10.1007/BF00186516.

[33] Bronkhorst IHG, Ly L V., Jordanova ES, Vrolijk J, Versluis M, Luyten GPM, et al. Detection of M2-Macrophages in Uveal Melanoma and Relation with Survival. Investig Opthalmology Vis Sci. 2011;52(2):643. https://doi.org/10.1167/iovs.10-5979.

[34] Mäkitie T, Summanen P, Tarkkanen A, Kivelä T. Tumor-infiltrating macrophages (CD68(+) cells) and prognosis in malignant uveal melanoma. Invest Ophthalmol Vis Sci. 2001;42(7):1414–21.

[35] Landreville S, Agapova OA, Hartbour JW. Emerging insights into the molecular pathogenesis of uveal melanoma. Futur Oncol. 2008;4(5):629–36. https://doi.org/10.2217/14796694.4.5.629.

[36] Huang DW, Sherman BT, Lempicki RA. Bioinformatics enrichment tools: Paths toward the comprehensive functional analysis of large gene lists. Nucleic Acids Res. 2009;37(1):1–13. https://doi.org/10.1093/nar/gkn923.

[37] Huang DW, Sherman BT, Lempicki RA. Systematic and integrative analysis of large gene lists using DAVID bioinformatics resources. Nat Protoc. 2009;4(1):44–57. https://doi.org/10.1038/nprot.2008.211.

SUPPLEMENTARY FIGURES AND TABLES

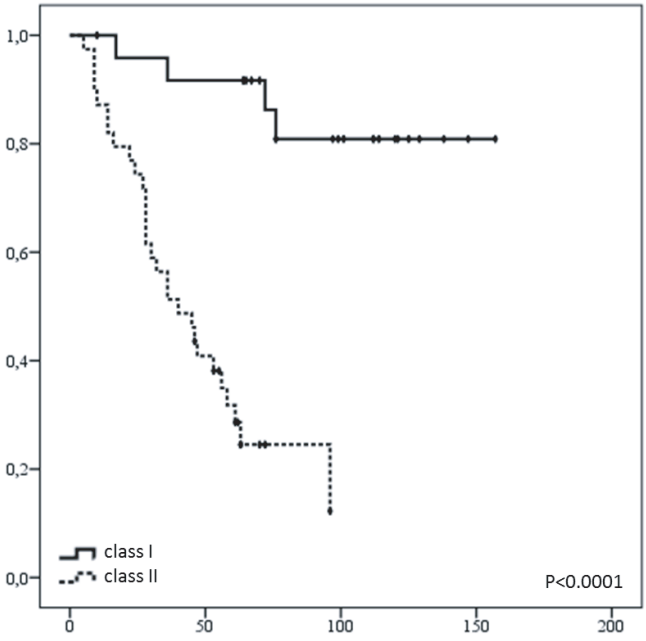

Figure S1, Kaplan-Meier analysis revealed a clear difference in survival between class I and class II.

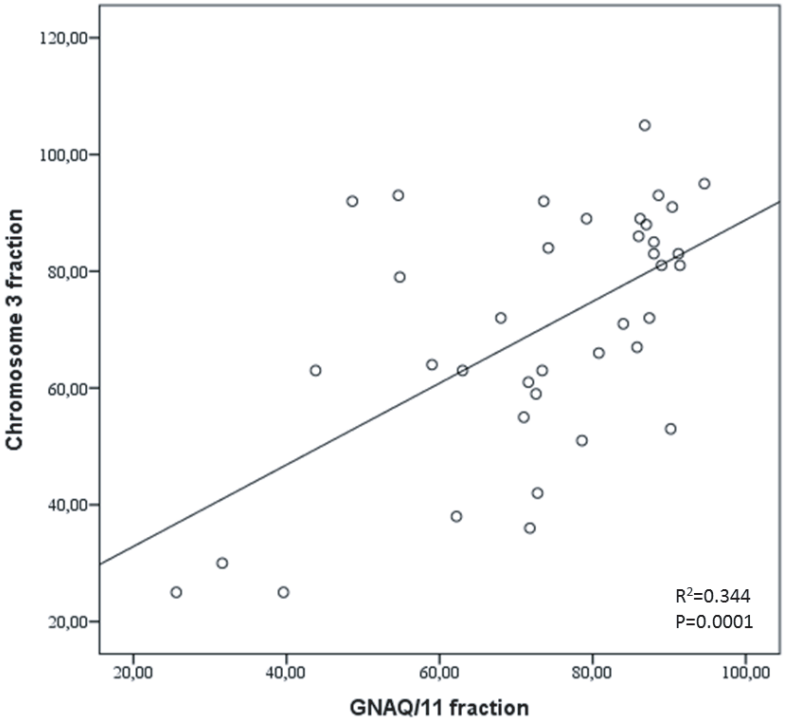

Figure S2, Correlation between fraction of tumor cells containing a GNAQ/11 mutation and fraction of tumor cells containing monosomy 3.
A significant correlation indicates that monosomy 3 fraction can be used to determine tumor-cell fraction in tumors which lack a GNAQ/11 mutation.

Table S1, dPCR sequence context.

Assay	MiQE Context Sequence
***GNAQ* Q209**	AGTGTATCCATTTTCTTCTCTCTGACCTTTGGCCCCCTACATCGACCATTCTGC AAGGTTAACAATACTCATATTAATAACATATAAAGTAAAACTAAAAAGTCAAC ATAAATATAGCACTAC
***GNA11* Q209**	CTTTCAGGATGGTGGATGTGGGGGGCCAGCGGTCGGAGCGGAGGAAGTGG ATCCACTGCTTTGAGAACGTGACATCCATCATGTTTCTCGTCGCCCTCAGCGA ATACGACCAAGTCCTGGTGG
TERT	CACCCCTTGGTGGCGGCTCACCTGTACGCCTGCAGCAGGAGGATCTTGTAGA TGTTGGTGCACACCGTCTGGAGGCTGTTCACCTAGAGTCGCCAAGAAAGAGT GAGAAACGGTAGAAACCTC
PPARG	TCTCCACCTTATTATTCTGAGAAGACTCAGCTCTACAATAAGCCTCATGAAG AGCCTTCCAACTCCCTCATGGCAATTGAATGTCGTGTCTGTGGAGATAAAGCT TCTGGATTTCACTATGGA
PTK2	CAACCAGATGGTCATTCAAAAAAGTTGGAGCTGTAAGTGCTGGCGACTGAG GACACAGGGTTAATTCCTCGCTGCTGGTGGAAGGCTAGAGAACATCTTCAAA AGAGGGTAGCAAGACGTGCT
CDC42	TTCACACACTTAGCTTTTTTTTGTGATGAGAACATTTAAAATATACTCACTTAG CAATTTTCAAGTGTGTAATACCGTATTATTAACTATAGTCACCATGCTGTACGG TAGCTCTCCAGAACG
NEDD9	GCTCCCCAGGCTGGAGTACAGTGGCACAATCTCAGCTTACAGCAACCTCTGC CTCCCGGGTTCAAGTGATTTTCCTGCCTCAGCCTCCTGAGTAGTTGAGATTA CAGGTGCACGCCACCATGC
NFAT5	TGGAAGCCATGAGAGAGAATATGATTTCAGGAAAACTTGGGCACAGAGAATT TGGCCTATCTCAGTATGACAAACTAATAGCTGTTGTGATTCATTTAGGGACTG TTGTTAAATATTTGATTA

Table S2, Gene expression of the top differentially expressed genes in the three classes.

Probe	Map	GeneSymbol	LogFC.1 vs 2	Adj. p-value 1 vs 2
ILMN_1735764	2q36.3-q37.1	HTR2B	-3.773908392	3.32E-14
ILMN_1803945	6p21.3	HCP5	-2.66663481	2.95E-10
ILMN_1778401	6p21.3	HLA-B	-2.38907834	2.45E-08
ILMN_1691641	Xq13.1	CITED1	-2.287132646	5.18E-10
ILMN_2337655	14q32.31	WARS	-2.266810219	4.91E-09
ILMN_1727271	14q32.31	WARS	-2.143112717	2.17E-08
ILMN_1770940	16q22.1	CDH1	-2.076563054	2.36E-07
ILMN_2058782	14q32	IFI27	-2.036064217	0.000495533
ILMN_1751079	6p21.3	TAP1	-1.999461061	3.00E-07
ILMN_2329735	1q21	ECM1	-1.996423647	4.22E-09
ILMN_2352097	16q13	GPR56	-1.978357632	1.40E-08
ILMN_1720282	16q22.1	NQO1	-1.958702811	7.01E-12
ILMN_1724533	8q21.11	LY96	-1.943487835	5.42E-05
ILMN_2384122	16q13	GPR56	-1.938534966	1.06E-08
ILMN_2188862	19p13.11	GDF15	-1.920898369	5.02E-06
ILMN_1657111	14q32.33	AHNAK2	-1.904421005	2.83E-07
ILMN_1691364	2q32.2	STAT1	-1.901311636	3.87E-06
ILMN_2186806	6p21.3	HLA-A	-1.856722458	1.24E-06
ILMN_1758128	17q25	CYGB	-1.849044334	2.74E-08
ILMN_2130441	6p21.3	HLA-H	-1.837938204	2.68E-07
ILMN_2049536	17p11.2	TRPV2	-1.726229181	3.32E-08
ILMN_2054019	1p36.33	ISG15	-1.710533103	1.79E-05
ILMN_1784602	6p21.2	CDKN1A	-1.637679023	6.72E-08
ILMN_3243156	14q32.33	AHNAK2	-1.631469761	4.57E-07
ILMN_1723978	22q13.1	LGALS1	-1.607783419	5.87E-11
ILMN_1801246	11p15.5	IFITM1	-1.603895174	7.09E-05
ILMN_1660691	18p11.3	RAB31	-1.582171721	2.07E-11
ILMN_2108735	20q13.3	EEF1A2	-1.581954568	0.003061057
ILMN_1676563	10q26.3	HTRA1	-1.571761855	1.06E-08
ILMN_1666078	6p21.3	HLA-H	-1.56693276	0.000220765
ILMN_1694268	2q37.3	HES6	-1.551730975	3.51E-10
ILMN_2379644	5q32	CD74	-1.522558292	0.000208917
ILMN_1704154	13q12.11-q12.3	TNFRSF19	-1.50147218	1.67E-07
ILMN_2060086	2q33	ADAM23	-1.494049148	1.24E-05
ILMN_2366330	11q13.1	FERMT3	-1.482467027	1.63E-08

LogFC.2A vs 2B	Adj.p-value 2A vs 2B	LogFC.1 vs 2A	Adj.p-value 1 vs 2A
-0.934860257	0.065334695	-3.199143842	1.15E-10
-1.526639411	0.00433641	-1.666679192	5.21E-05
-2.081580926	0.000862178	-1.03733205	0.018977868
-0.171011652	0.585474286	-2.167603733	6.73E-07
-1.805074178	0.000158268	-1.194667337	0.000551673
-1.780051251	0.000301266	-1.064401571	0.00231439
0.867038878	0.044872618	-2.652152735	7.75E-08
-2.952315446	0.000341596	-0.053944659	0.964550758
-2.17396159	1.55E-05	-0.713550773	0.04172581
-0.862975474	0.097090624	-1.432839125	7.84E-05
0.06638202	0.880409419	-2.089506775	5.00E-07
-0.312744968	0.456598454	-1.744600311	3.40E-08
-1.61796231	0.026150643	-0.727712908	0.303492543
0.080961406	0.84253637	-2.057689005	3.03E-07
-0.689602297	0.218668928	-1.386779452	0.009212452
0.19839201	0.79063382	-1.967675258	4.25E-05
-2.22685769	0.000156814	-0.519941698	0.268249908
-1.842512556	0.000548884	-0.680184582	0.125312752
-0.134359598	0.839360217	-1.877894072	2.25E-06
-1.827910037	5.54E-05	-0.661482354	0.091379956
-0.226198045	0.745153761	-1.49996204	9.93E-05
-2.218751047	5.35E-05	-0.342756166	0.480783875
-0.382698788	0.549429049	-1.305559946	0.001062968
0.245578987	0.676536857	-1.717288078	4.15E-05
-0.597722926	0.040683991	-1.13374455	0.000225399
-2.172972454	5.54E-05	-0.2908723	0.609435438
-0.163211795	0.677888809	-1.401483179	5.75E-07
-1.256779356	0.143336167	-0.812554953	0.294247268
-0.281216032	0.578241003	-1.25839444	0.00029402
-1.492089818	0.011779147	-0.804267994	0.118692468
0.010207587	0.987060183	-1.389314129	1.94E-05
-1.456207652	0.05047505	-0.575269248	0.352677712
-0.17432277	0.810775999	-1.3172177	0.000305706
0.892425379	0.099186067	-2.080566429	1.36E-06
-0.155069949	0.726916522	-1.323238034	4.78E-05

Table S2, Gene expression of the top differentially expressed genes in the three classes. (continued)

Probe	Map	GeneSymbol	LogFC.1 vs 2	Adj. p-value 1 vs 2
ILMN_1725427	15q21-q22.2	B2M	-1.481512737	3.54E-07
ILMN_1679208	7q22.1	LHFPL3-AS1	-1.477219872	4.57E-07
ILMN_1736567	5q32	CD74	-1.475482233	0.000347899
ILMN_2148459	15q21-q22.2	B2M	-1.474818568	1.09E-08
ILMN_2390299	6p21.3	PSMB8	-1.462913166	3.24E-07
ILMN_1653494	1q21	S100A1	-1.456593391	0.000100276
ILMN_1793476	11p15.4	PRKCDBP	-1.419121924	5.40E-07
ILMN_1747195	6p21.3	PSMB8	-1.406736629	2.33E-07
ILMN_1796409	1p36.12	C1QB	-1.40534744	0.000681717
ILMN_1659913	15q26	ISG20	-1.403091805	3.91E-05
ILMN_1725193	2q33-q34	IGFBP2	-1.399708363	3.09E-08
ILMN_1782050	8p11.2-p11.1	CEBPD	-1.395006423	4.39E-07
ILMN_2157441	6p21.3	HLA-DRA	-1.393274828	0.001410494
ILMN_1769779	8q24.3	PTP4A3	-1.39004584	1.31E-07
ILMN_1762861	6p21.3	HLA-F	-1.351637038	1.98E-05
ILMN_1708375	5q31.1	IRF1	-1.343649903	3.26E-05
ILMN_1810844	7q36.1	RARRES2	-1.335158883	0.000222874
ILMN_1765258	6p21.3	HLA-E	-1.311146182	7.66E-06
ILMN_1772218	6p21.3	HLA-DPA1	-1.310768829	0.002836507
ILMN_1729691	17q24.2	SLC16A6	-1.299771314	3.62E-06
ILMN_1713636	1q21	S100A6	-1.294152227	2.53E-07
ILMN_1702487	6q23	SGK1	-1.291490458	0.001490199
ILMN_2109708	22q13.33	TYMP	-1.2878876	2.21E-05
ILMN_1795930	5p13.1	PTGER4	-1.286717865	0.000970005
ILMN_2098126	17q11.2-q12	CCL5	-1.284655576	0.002322207
ILMN_2358069	7p22	MAD1L1	-1.274162082	1.04E-08
ILMN_2359710	8q24.3	PTP4A3	-1.273250293	2.03E-07
ILMN_1696187	14q21-q22	PYGL	-1.254681852	0.001771987
ILMN_1730084	22q11.21	COMT	-1.253157567	5.73E-12
ILMN_1806733	21q22.3	COL18A1	-1.248432723	4.63E-09
ILMN_1785902	1p36.11	C1QC	-1.242953802	0.000337762
ILMN_1761733	6p21.3	HLA-DMB	-1.23681126	0.001074151
ILMN_1739241	15q15.1	CHAC1	-1.233630321	4.86E-11
ILMN_1757387	4p14	UCHL1	-1.223234587	0.000958245
ILMN_1669523	14q24.3	FOS	-1.22144887	0.000151106

LogFC.2A vs 2B	Adj.p-value 2A vs 2B	LogFC.1 vs 2A	Adj.p-value 1 vs 2A
-1.27677156	0.002141	-0.667950409	0.035732787
-0.498307113	0.329942711	-1.000683167	0.005230774
-1.451771578	0.054889055	-0.528228843	0.412408716
-1.128232399	0.000518798	-0.733307622	0.005499572
-1.489399362	5.54E-05	-0.464486376	0.127891696
0.108023535	0.895535539	-1.615577519	0.000696915
-0.412504148	0.449002125	-1.026111852	0.00681702
-1.361023129	0.000142967	-0.484940728	0.090678383
-1.495300525	0.026994241	-0.448802397	0.484071008
-1.549345257	0.00060989	-0.306617422	0.478974807
-0.12908906	0.843863729	-1.162161451	0.000466155
-0.043338611	0.952858182	-1.334197316	0.000210616
-1.738923346	0.014976541	-0.282501616	0.717775178
-0.484935905	0.252641849	-1.100111001	0.000280978
-1.385331383	0.003045645	-0.350139811	0.41508905
-1.432841362	0.001588993	-0.381627053	0.34522034
-0.062936549	0.944543429	-1.165391772	0.022203596
-1.611888624	0.000158268	-0.315797125	0.409305273
-1.453661429	0.061661454	-0.357607473	0.640730802
-0.090602799	0.913423939	-1.231147812	0.000626107
-0.638913429	0.120437702	-0.895606445	0.00325878
-0.294082571	0.718613535	-0.928152744	0.129251968
-1.512205093	0.000283042	-0.327015501	0.446610528
-0.76748395	0.18230754	-0.606010589	0.336703663
-1.86024864	0.008616187	-0.060827329	0.948879493
0.081873277	0.89705128	-1.250656388	1.11E-05
-0.419965606	0.335068999	-1.002959441	0.000564678
0.453479289	0.60410177	-1.648594315	0.001355887
0.298837526	0.245428188	-1.398281728	4.04E-10
-0.13563169	0.807207586	-1.09196204	4.15E-05
-1.292361987	0.017742391	-0.423036425	0.392003425
-1.409926005	0.016646807	-0.208680975	0.783227001
-0.097759854	0.807164842	-1.153413343	4.53E-07
-0.627741177	0.217766395	-0.485457064	0.453521545
-0.264449692	0.721002588	-1.057807158	0.012502918

Table S2, Gene expression of the top differentially expressed genes in the three classes. (continued)

Probe	Map	GeneSymbol	LogFC.1 vs 2	Adj. p-value 1 vs 2
ILMN_1682928	7p15.1	CPVL	-1.213052895	2.24E-08
ILMN_2062468	4q12	IGFBP7	-1.212651879	3.52E-05
ILMN_1786041	Xp22.2	ASB9	-1.209130965	5.63E-08
ILMN_1779171	17p13.3	SGSM2	-1.20596083	5.37E-07
ILMN_1662427	8q24.3	PTP4A3	-1.205823574	3.09E-07
ILMN_1671054	6p21.3	HLA-A	-1.205252456	4.13E-07
ILMN_1662358	21q22.3	MX1	-1.203899161	0.000440498
ILMN_1687384	1p35	IFI6	-1.198258771	0.000442643
ILMN_1663866	5q31	TGFBI	-1.189847867	3.17E-06
ILMN_1656194	17q25.3	TSPAN10	-1.188484584	4.56E-06
ILMN_1777325	2q32.2	STAT1	-1.18802805	0.000202326
ILMN_1676099	4p16.3	SPON2	-1.177578697	3.55E-09
ILMN_2229379	4q11-q12	KIT	-1.176612669	0.000936995
ILMN_1789733	19q13.12	CLIP3	-1.171904708	1.50E-06
ILMN_1689655	6p21.3	HLA-DRA	-1.167043216	0.007892476
ILMN_1710740	6p21.3	C2	-1.164851011	6.17E-10
ILMN_1801766	4q25	CCDC109B	-1.163072045	6.52E-08
ILMN_1790160	4q11-q12	KIT	-1.161790871	0.002217089
ILMN_1656670	6p21.3	HLA-G	-1.155427467	7.79E-06
ILMN_2366212	17q23	CD79B	-1.152695659	3.99E-05
ILMN_2400759	7p15.1	CPVL	-1.152219072	1.24E-07
ILMN_1805750	11p15.5	IFITM3	-1.146116484	3.97E-08
ILMN_1688780	1q21	S100A4	-1.145891451	0.000928153
ILMN_2203950	6p21.3	HLA-A	-1.145672159	3.38E-09
ILMN_1690105	2q32.2	STAT1	-1.143448518	0.000309827
ILMN_1771800	17q22-q23.2	PRKCA	-1.124829082	4.51E-05
ILMN_2067656	12p13	CCND2	-1.120127725	0.004083695
ILMN_1774077	1p22.2	GBP2	-1.117392306	0.004043561
ILMN_1815115	8q24.3	CYC1	-1.111580082	4.63E-08
ILMN_1722820	22q13.1	KDELR3	-1.110198917	4.14E-08
ILMN_1808405	6p21.3	HLA-DQA1	-1.107343321	0.015565072
ILMN_1802027	4q28.3	MGST2	-1.101678462	1.06E-08
ILMN_1695311	6p21.3	HLA-DMA	-1.094127489	0.000890934
ILMN_1743103	10q24.33	SH3PXD2A	-1.08906427	3.38E-06
ILMN_2334296	11q13	IL18BP	-1.082418546	0.00016257

LogFC.2A vs 2B	Adj.p-value 2A vs 2B	LogFC.1 vs 2A	Adj.p-value 1 vs 2A
-0.199378838	0.415111615	-1.158055933	2.09E-06
0.217779953	0.677086483	-1.451266092	7.88E-05
0.282118814	0.488074948	-1.441938823	1.10E-07
0.432776886	0.122474351	-1.583182598	5.85E-08
-0.415432091	0.296312507	-0.941502922	0.000743735
-1.033963813	0.001992219	-0.434241785	0.150599387
-1.673818424	0.002630017	-0.189552499	0.769106644
-1.847146326	0.000301266	-0.04565734	0.953193267
-0.508328367	0.290550661	-0.869434873	0.005514915
0.150583817	0.773596208	-1.310845191	0.000128899
-1.895540123	5.54E-05	0.003009297	0.996141387
-0.177833628	0.686698836	-0.933368764	0.00034736
0.735803564	0.176446393	-1.815791705	0.000101932
0.161867421	0.730052968	-1.159783617	0.000639028
-1.613776991	0.027715304	-0.135281356	0.878552409
-0.424882045	0.098916056	-0.871550238	2.21E-05
-0.504777282	0.109892945	-0.701162306	0.00977496
0.963724842	0.104580216	-1.901990254	0.000231025
-1.153720079	0.000555697	-0.403899161	0.196509477
-0.252558905	0.636624936	-1.083677951	0.002516523
-0.219539557	0.405082416	-1.107281891	1.03E-05
-0.665509972	0.015898115	-0.727714558	0.002113514
-0.8091866	0.132261453	-0.569235362	0.264284082
-0.779088685	0.000856288	-0.641404042	0.002494604
-1.36174288	0.002120612	-0.180381399	0.709423443
-0.3701347	0.503222467	-0.903227909	0.011468085
0.475659118	0.420139451	-1.418441381	0.006122274
-1.715583799	0.00433641	0.004970278	0.995396575
-0.554010798	0.108902369	-0.76621322	0.000989067
-0.370423955	0.18281206	-0.905728416	5.90E-05
-1.444103747	0.054603468	-0.095545379	0.922552961
-0.361167552	0.12459274	-0.929274922	1.07E-05
-1.352001983	0.009311445	-0.225074599	0.709598127
0.607414723	0.137438736	-1.400508743	3.78E-06
-1.191449854	0.002971623	-0.201727242	0.679569868

Table S2, Gene expression of the top differentially expressed genes in the three classes. (continued)

Probe	Map	GeneSymbol	LogFC.1 vs 2	Adj. p-value 1 vs 2
ILMN_2066066	6p21.3	HLA-DRB6	-1.081050989	0.004337548
ILMN_1708778	9q34.1	ASS1	-1.07728373	2.91E-05
ILMN_1803788	14q22.3	LGALS3	-1.070982922	1.04E-05
ILMN_1673352	11p15.5	IFITM2	-1.070116856	1.12E-08
ILMN_3245057	8q24.1-q24.2	ASAP1	-1.068044193	5.13E-07
ILMN_3305938	6q23	SGK1	-1.064550475	0.007636294
ILMN_1805737	10p15.3-p15.2	PFKP	-1.064253058	1.13E-07
ILMN_1684306	1q21	S100A4	-1.055266309	0.001034069
ILMN_1686664	16q13	MT2A	-1.050536453	0.00018572
ILMN_1745034	12q13	SLC11A2	-1.045247158	3.87E-08
ILMN_1787345	12q13.12	FKBP11	-1.044617402	0.000305274
ILMN_1701613	11q23	RARRES3	-1.04129153	0.028213669
ILMN_1771652	22q13.1	BAIAP2L2	-1.037245324	9.58E-07
ILMN_1743836	17q25.1	MXRA7	-1.035744309	9.22E-11
ILMN_1656920	14q32.33	CRIP1	-1.035138968	6.35E-07
ILMN_1766657	9q34.1	STOM	-1.032720922	8.73E-07
ILMN_1778977	19q13.1	TYROBP	-1.026783881	0.004074888
ILMN_3229324	6q23	SGK1	-1.017792894	0.015168731
ILMN_2218208	4q22.1	SPARCL1	-1.016969117	0.026934898
ILMN_1744118	9q33.1	ASTN2	-1.013255179	1.37E-05
ILMN_1736982	6p24.1	PHACTR1	-1.010594848	0.047662066
ILMN_1676893	2p23.3	ADCY3	-1.010294916	2.34E-08
ILMN_1725791	10p14-p13	PTPLA	-1.010177268	8.73E-07
ILMN_1773352	17q11.2-q12	CCL5	-1.010089785	0.002187047
ILMN_2376108	6p21.3	PSMB9	-1.00615672	0.000970071
ILMN_1723480	19p13.1	BST2	-1.00536494	0.002547297
ILMN_1732923	1q42.2	SIPA1L2	-1.001007275	7.61E-09
ILMN_2227817	6p12.1	GSTA3	1.000389382	0.007978159
ILMN_3210171	1q32.3	RPL21P28	1.009169659	2.01E-05
ILMN_2230025	4q35	PDLIM3	1.012908713	0.000827357
ILMN_1729033	4p13	RPL9	1.01384583	3.88E-08
ILMN_3225591	3p22-p21.2	RPL14	1.020358629	1.14E-12
ILMN_1691611	19p13.2	HNRNPA1P10	1.025336757	2.74E-08
ILMN_3304898	6p21.33	TUBB	1.025842056	5.31E-08
ILMN_1699562	8q11.21	EFCAB1	1.026617421	0.000220765

LogFC.2A vs 2B	Adj.p-value 2A vs 2B	LogFC.1 vs 2A	Adj.p-value 1 vs 2A
-1.420112933	0.019127522	-0.106183998	0.892864946
-0.364980639	0.368764337	-0.637488249	0.095475721
-0.822964131	0.011779147	-0.480980901	0.155314416
-0.698340489	0.004154219	-0.653207814	0.00146188
0.251282236	0.565761753	-1.172244835	2.41E-05
-0.290727373	0.710479608	-0.690151371	0.274836645
-0.281986458	0.227127929	-0.842631468	0.00049186
-0.769577479	0.103832364	-0.507951039	0.285227807
-0.813068892	0.060627835	-0.496255256	0.207895987
-0.100349454	0.822909956	-0.953501469	8.71E-05
-0.615553014	0.254352932	-0.691177225	0.094597515
-2.117220714	0.001197527	0.359788873	0.590200319
0.08336743	0.83299303	-1.186731927	3.83E-06
0.122853077	0.718989023	-1.066988757	6.25E-08
-0.571091783	0.091294504	-0.610058978	0.018735274
-0.686220443	0.03717254	-0.5476821	0.043531095
-1.285362278	0.012378171	-0.056575673	0.945469006
-0.271510437	0.748202438	-0.63921103	0.349488079
0.840276126	0.405034431	-1.532358514	0.010204208
-0.038780848	0.957168549	-0.983087258	0.001245753
-0.495126318	0.535259965	-0.58128186	0.494308796
-0.196587678	0.521295588	-0.7775104	0.001426401
-0.19282835	0.678530722	-0.874405961	0.000700149
-1.247163489	0.022681411	-0.082984494	0.903532691
-1.245073429	0.003045645	-0.001525824	0.998188548
-1.616081005	0.000486479	0.067795293	0.912632742
0.248899188	0.354864633	-1.221156841	1.98E-08
0.32219132	0.283738698	0.885142665	0.091525165
-0.043780051	0.956450371	0.925899886	0.005180224
0.118682307	0.832217916	0.969901392	0.032247858
0.106650368	0.836323157	0.912498289	0.000670585
0.254346968	0.199791869	0.84168109	3.68E-08
0.409599232	0.209889412	0.647860311	0.011950508
0.256964706	0.344464336	0.797557368	0.00151551
0.063224105	0.480255267	1.020701496	0.004029976

Table S2, Gene expression of the top differentially expressed genes in the three classes. (continued)

Probe	Map	GeneSymbol	LogFC.1 vs 2	Adj. p-value 1 vs 2
ILMN_1774823	4q25	RPL34	1.03941488	1.56E-08
ILMN_3278506	7p15.3	RPS2P32	1.040920931	1.21E-06
ILMN_2325506	20q13.13	BCAS4	1.043939436	1.82E-05
ILMN_1740927	6p25.1	LYRM4	1.046906568	2.07E-11
ILMN_2389273	3q28	FXR1	1.047553084	1.04E-10
ILMN_1766165	4q21	SNCA	1.051796428	5.47E-06
ILMN_1654609	5q22.2	EPB41L4A-AS1	1.054896923	1.60E-08
ILMN_1797154	7q22.1	AZGP1	1.057343839	2.84E-08
ILMN_1808059	20q13.13	BCAS4	1.058574197	5.55E-06
ILMN_1741096	8p23.1-p22	FDFT1	1.066405633	8.09E-07
ILMN_3293685	16p13.3	RPS2	1.072483613	4.54E-06
ILMN_1679093	19q13.42	ZNF581	1.072600242	1.67E-10
ILMN_1665824	6p24.3	LINC00518	1.074925305	4.20E-08
ILMN_3302177	3p22-p21.2	RPL14	1.077184959	3.36E-11
ILMN_1680344	18p11.31	MYOM1	1.078054364	0.000271898
ILMN_1808041	6p21.31	RPL10A	1.082382125	3.29E-06
ILMN_1654946	19q13.43	ZSCAN18	1.082955746	4.22E-09
ILMN_2144088	8p23.1-p22	FDFT1	1.086032559	2.37E-06
ILMN_1664292	19q13.42	ZNF415	1.088629313	2.40E-14
ILMN_2351638	Xq22.1-q22.3	BEX4	1.08871681	3.42E-10
ILMN_2138765	9p22.1	PLIN2	1.0950394	3.00E-08
ILMN_1679640	3q28	FXR1	1.0988054	2.31E-12
ILMN_1810533	12q21.3	SLC6A15	1.100594841	1.90E-08
ILMN_1766446	6p21.3	C6orf48	1.100937012	3.25E-09
ILMN_1660439	22q13	RPL3	1.106517102	1.76E-07
ILMN_3244583	5q22.2	EPB41L4A-AS1	1.108311628	6.78E-09
ILMN_1694106	3p22.3	GPD1L	1.110684568	1.10E-09
ILMN_3225784	9q21.13	RPSAP9	1.114453354	4.02E-10
ILMN_2404850	3p22-p21.2	RPL14	1.128421289	0.000912076
ILMN_3241051	3p25-p24	RPL32	1.144777125	1.68E-11
ILMN_1762747	3p24.2	RPL15	1.147236254	6.16E-11
ILMN_1717381	2q31.1	HOXD1	1.149018854	0.001869334
ILMN_1742330	3p21.31	PLXNB1	1.151634332	4.77E-09
ILMN_1765574	6p24	TFAP2A	1.155987834	3.47E-06
ILMN_1808837	9q34	RPL7A	1.157624855	4.61E-09

LogFC.2A vs 2B	Adj.p-value 2A vs 2B	LogFC.1 vs 2A	Adj.p-value 1 vs 2A
0.093231041	0.789770273	0.964168005	0.000221881
0.177597564	0.747809982	0.894309529	0.004914792
-0.183413303	0.608029491	1.273257967	2.78E-05
0.242269164	0.109745518	0.88699802	1.47E-07
0.215593781	0.102435441	0.88530183	3.31E-06
0.28018814	0.302800751	0.864838221	0.003237044
0.538245025	0.083463239	0.649568228	0.008895082
0.178031986	0.120437702	0.907332771	4.34E-05
-0.137182546	0.68512161	1.263332358	1.05E-05
0.525631817	0.170094483	0.68629575	0.012896564
0.093858595	0.905768961	0.923115148	0.005843499
0.197124122	0.335375027	0.888933663	2.15E-05
0.149632708	0.366535017	0.771126237	0.005119079
0.241119376	0.368764337	0.930657812	8.95E-07
-0.087273802	0.664111921	1.201942327	0.001839539
0.195958938	0.747678818	0.89521463	0.004843674
0.279033998	0.385037485	0.884732152	4.91E-05
0.608412996	0.149593528	0.704375182	0.01383804
-0.060568205	0.450118757	1.173901165	1.41E-14
0.266483391	0.258920998	0.870348102	2.78E-05
-0.341854853	0.24190242	1.366876809	1.98E-08
0.266476463	0.080969607	0.944250501	3.48E-09
0.335476464	0.213403899	0.826079503	0.000784998
0.226332046	0.340211668	0.927314751	2.67E-05
0.40250656	0.263954692	0.763851676	0.006599111
0.545709662	0.055987692	0.692940462	0.004698967
0.392620984	0.047867867	0.823978019	4.25E-05
0.209152773	0.435478729	1.028823175	1.61E-07
0.477220804	0.382725969	0.648983261	0.207973525
0.377499734	0.081451755	0.896340608	6.54E-07
0.485573398	0.035493668	0.834717513	1.32E-05
-0.016326993	0.979370587	1.257530218	0.010351204
0.307456076	0.156975198	0.986064207	3.14E-06
0.894639838	0.00485557	0.64083042	0.021720434
0.387443005	0.109745518	0.794960725	0.002820649

Table S2, Gene expression of the top differentially expressed genes in the three classes. (continued)

Probe	Map	GeneSymbol	LogFC.1 vs 2	Adj. p-value 1 vs 2
ILMN_3243291	12q13.1	HNRNPA1	1.168422696	5.16E-08
ILMN_3294222	7p15.3	RPS2P32	1.184870421	8.70E-06
ILMN_3274596	3q28	EIF4A2	1.185844732	1.68E-08
ILMN_2181892	Xq22	BEX2	1.18895458	3.01E-07
ILMN_1758049	1p31.3-p31.2	NFIA	1.196694805	5.29E-11
ILMN_1793990	2p25	ID2	1.204169896	3.69E-07
ILMN_1672503	8p22-p21	DPYSL2	1.204618695	5.30E-06
ILMN_3243616	20q13.33	LOC100127888	1.216677914	5.32E-06
ILMN_3309349	4q26	SNHG8	1.217538898	0.000687661
ILMN_1775743	12q22	BTG1	1.227172139	2.34E-07
ILMN_1732154	1q31	BCAN	1.234925957	0.000329621
ILMN_2146389	5q33	MEGF10	1.244835792	1.36E-10
ILMN_1713529	5q23.1	SEMA6A	1.245867424	5.97E-06
ILMN_1690342	12q22	LTA4H	1.247267616	2.31E-12
ILMN_1684982	7q21.3	PDK4	1.272845665	1.11E-05
ILMN_1655422	18q21	RPL17	1.278107874	5.41E-08
ILMN_1685917	4q24	EMCN	1.278180642	1.09E-07
ILMN_1751904	13q22	EDNRB	1.280184833	0.000167768
ILMN_1740234	10q25.1	GSTO2	1.289190898	1.75E-05
ILMN_1658498	1p21.3	SLC44A3	1.291554929	6.26E-09
ILMN_1716014	3p24.2	RPL15	1.294050275	8.81E-09
ILMN_3287068	9q21.13	RPSAP9	1.30214539	1.73E-10
ILMN_1692058	15q11.2-q12	NDN	1.30284313	2.29E-06
ILMN_1790881	2q22.1	HNMT	1.305607283	1.12E-08
ILMN_1754969	3p26-p24	LMCD1	1.313718501	4.86E-11
ILMN_1733305	3q25.1	EIF2A	1.315492384	3.32E-14
ILMN_1785424	10q25	ABLIM1	1.319568054	1.30E-05
ILMN_1671554	2p25.1	LPIN1	1.320195822	4.10E-10
ILMN_1691053	16p13.3	RPS2	1.337410651	6.42E-09
ILMN_1772627	4p16.3	NSG1	1.339033154	4.83E-08
ILMN_1682459	19p13.3	TUBB4A	1.351559415	3.03E-07
ILMN_3227023	9q34.3	SNHG7	1.365658127	2.11E-08
ILMN_1679324	3p22.1	EIF1B	1.399790804	7.99E-11
ILMN_1712786	7q32.1	AHCYL2	1.406766726	7.62E-07
ILMN_1736670	10q23-q24	PPP1R3C	1.41282522	1.45E-05

LogFC.2A vs 2B	Adj.p-value 2A vs 2B	LogFC.1 vs 2A	Adj.p-value 1 vs 2A
0.379313703	0.339819137	0.794206907	0.00808425
0.512576125	0.231290236	0.670509356	0.09278963
0.081121203	0.881125075	1.117905095	2.20E-05
-0.000435374	0.998680003	1.163167865	8.68E-05
0.129687319	0.120214425	1.088415295	2.55E-08
0.119990511	0.723833155	1.235304813	4.16E-06
0.308264815	0.574172971	1.094493565	0.000820227
0.665181424	0.054251792	0.715201734	0.061915381
0.283230754	0.711384187	0.981324303	0.048967414
0.27512776	0.542971946	1.06785611	0.000259036
0.092682046	0.859477273	1.23256803	0.005531251
0.018019419	0.80518906	1.199536868	2.11E-07
1.073177232	0.001992219	0.593865104	0.056583351
0.279998099	0.14712732	1.09837339	1.85E-09
0.096661757	0.689596535	1.098202322	0.006094742
-0.07032434	0.910619571	1.349116661	1.47E-05
0.056026727	0.915318731	1.212684394	0.000370253
0.960543451	0.048334041	0.739750872	0.09122889
0.093163282	0.796473023	1.151420901	0.003569825
0.461201737	0.037553517	0.813982711	0.003691123
0.135250391	0.780674971	1.208660273	1.11E-05
0.188443385	0.505045669	1.218323469	1.07E-07
0.032000201	0.974399337	1.299779461	0.0002229
0.243631764	0.457196304	1.187279893	6.88E-06
0.016442545	0.910393484	1.346172489	1.85E-09
0.313502771	0.03359472	1.070634923	6.06E-08
0.372574362	0.166192781	1.14573872	0.002051582
0.360134813	0.129333387	1.065648353	6.28E-06
0.245972769	0.453571352	1.092622198	0.000327466
0.41835911	0.179117132	1.140256143	0.000119501
0.738871781	0.006675471	0.965868934	0.000481317
0.806325225	0.056357312	0.858783102	0.003469886
-0.095756672	0.831345998	1.444967125	2.93E-08
0.35055169	0.490113011	1.162861731	0.00092869
0.96377997	0.002052965	0.79295205	0.051301141

Table S2, Gene expression of the top differentially expressed genes in the three classes. (continued)

Probe	Map	GeneSymbol	LogFC.1 vs 2	Adj. p-value 1 vs 2
ILMN_3289100	3p21.3-p21.2	RPL29	1.424227229	5.53E-10
ILMN_2374115	6p24	TFAP2A	1.427376215	4.22E-09
ILMN_2218935	7q31	GPR37	1.454469504	2.02E-05
ILMN_3233229	9q34.3	SNHG7	1.461632818	4.77E-08
ILMN_1807050	15q21.1-q21.2	SHC4	1.463334644	8.75E-09
ILMN_1687978	12q15	PHLDA1	1.507837374	3.37E-09
ILMN_2176592	3q26.1-q26.2	BCHE	1.510293282	4.95E-11
ILMN_3226291	3p21.3-p21.2	RPL29	1.518659314	1.91E-10
ILMN_1751346	12q13	ERBB3	1.533761351	3.27E-08
ILMN_1701933	4q21	SNCA	1.540994797	4.27E-06
ILMN_1659550	12q14.3	RPSAP52	1.626872445	2.02E-07
ILMN_3219764	3p22.2	RPSA	1.632917134	4.86E-11
ILMN_1781758	3q21.2	ROPN1B	1.636828911	6.44E-11
ILMN_1780799	8q24.1	ENPP2	1.707714414	5.06E-06
ILMN_2373791	8q24.1	ENPP2	1.707933561	6.62E-06
ILMN_1741404	8q21	MSC	1.713599687	2.22E-06
ILMN_3268403	19q13.43	LOC100128252	1.73596967	2.65E-15
ILMN_1726460	3p22-p21.2	RPL14	1.810952692	2.66E-13
ILMN_1703572	13q21	PCDH20	1.814353409	1.06E-06
ILMN_3307906	1p22-p21	PALMD	1.961562592	3.74E-08
ILMN_2344120	3q21.2	ROPN1B	1.966947982	5.29E-11
ILMN_1668766	3q21.1	ROPN1	2.0412616	4.86E-11
ILMN_2166457	4q34-q35	HPGD	2.082430064	4.76E-10
ILMN_1733860	3p14.2	SYNPR	2.295113339	1.43E-07
ILMN_1749875	12p13.31	LOC728715	2.403788128	7.54E-08
ILMN_2374449	4q22.1	SPP1	2.557887027	3.52E-05
ILMN_1651354	4q22.1	SPP1	2.607482094	7.67E-05

LogFC.2A vs 2B	Adj.p-value 2A vs 2B	LogFC.1 vs 2A	Adj.p-value 1 vs 2A
0.407122491	0.223840114	1.151857458	1.92E-05
0.628374495	0.005203369	0.993976042	0.000183433
0.872541243	0.035064285	0.739604938	0.124983922
0.759171839	0.078824777	0.92004441	0.006157917
0.020460022	0.925436808	1.488818569	8.90E-07
0.511392248	0.067518294	1.309639231	5.43E-07
0.134085017	0.602893484	1.261652892	1.37E-05
0.481222714	0.132924077	1.184637718	1.32E-05
0.825608838	0.025235833	0.909270118	0.005950394
0.511236896	0.354547349	1.266961361	0.00231439
0.077636637	0.933596867	1.580409429	6.17E-05
0.316400233	0.404253808	1.482346609	1.34E-07
0.078094634	0.763868135	1.595439593	5.09E-08
0.327647641	0.395114959	1.680884421	0.000104187
0.358956114	0.354138992	1.649444827	0.000181608
-0.045935557	0.850037685	1.982108139	8.39E-06
0.063595835	0.808209561	1.607147123	8.90E-11
0.420072629	0.104764819	1.442303419	1.34E-07
0.178842659	0.464299956	1.481972865	0.004839451
-0.006321993	0.968956764	2.054763961	1.24E-06
0.202607827	0.553888801	1.843453117	7.49E-08
0.156561029	0.632441945	1.953367657	2.93E-08
0.007126048	0.967369229	2.047051746	6.91E-07
0.418079902	0.312398369	2.034535612	5.53E-05
1.172083628	0.006374597	1.622884723	0.001103957
-0.560528642	0.432466398	3.204139236	3.00E-05
-0.709302937	0.426138115	3.293710762	7.04E-05

Table S3, Distribution of chromosomal imbalances over the three expression classes.

Aberration	Total (64)	Class I (25)	Class IIa (14)	Class IIb (25)	Class I vs. II	Class I vs. IIa	Class IIa vs. IIb	Class I vs IIb
8q								
-Normal	14	13	1	0	p<0.0001	p=0.005	p=0.148*	p<0.0001
-Trisomy	23	8	7	8	p=0.001	p=0.013*	p=0.228*	p=0.001*
-Amplification	27	4	6	17	p=0.001	p=0.069*	p=0.126	p=0.0002
Monosomy 3	41	3	13	25	p<0.0001	p<0.0001	p=0.148	p<0.0001
Gain 6p	43	23	8	12	p=0.001	p=0.01*	p=0.584	p=0.001
Loss 1p36	37	15	8	14	p=0.777	p=0.862	p=0.945	p=0.774
Loss 16q	21	9	2	10	p=0.664	p=0.134*	p=0.083*	p=0.771

** Likelihood ratio's*